Advances in Polymer Technology

Polymers for Membrane Separation

Lead Guest Editor: Xiao-Long Han
Guest Editors: Na Li and Zongli Xie

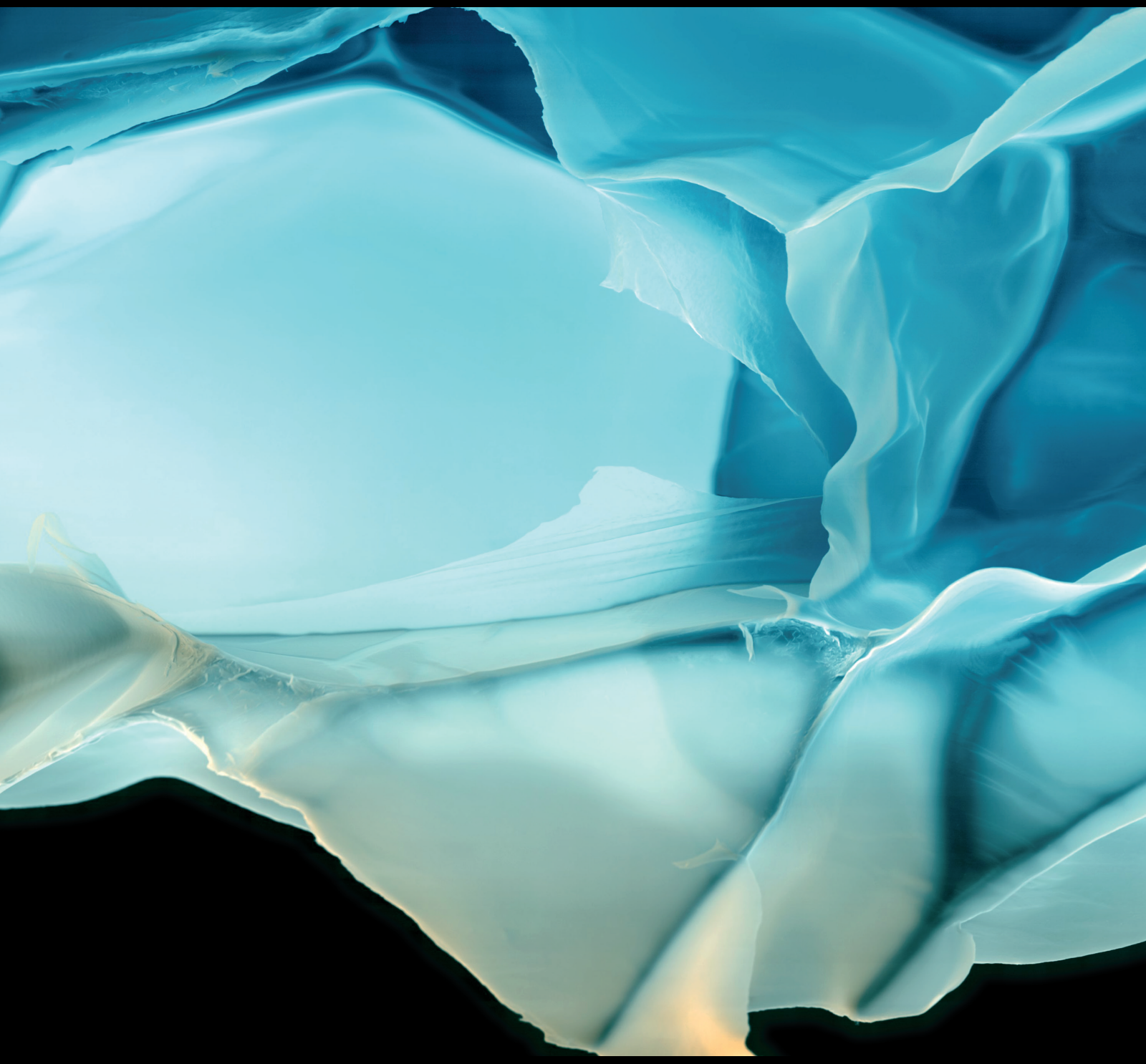

Polymers for Membrane Separation

Advances in Polymer Technology

Polymers for Membrane Separation

Lead Guest Editor: Xiao-Long Han
Guest Editors: Na Li and Zongli Xie

Contents

Hindawi
Advances in Polymer Technology
Volume 2019, Article ID 9692859, 15 pages
https://doi.org/10.1155/2019/9692859

Research Article

Fabrication of PES/PVP Water Filtration Membranes Using Cyrene®, a Safer Bio-Based Polar Aprotic Solvent

Roxana A. Milescu,[1] C. Robert McElroy,[1] Thomas J. Farmer,[1] Paul M. Williams,[2] Matthew J. Walters,[2] and James H. Clark[1]

[1]*Green Chemistry Centre of Excellence, Department of Chemistry, University of York, Heslington, York YO10 5DD, UK*
[2]*Department Chemical Engineering, Swansea University, Sketty, Swansea SA2 8PP, UK*

Correspondence should be addressed to James H. Clark; james.clark@york.ac.uk

Received 13 March 2019; Revised 29 May 2019; Accepted 11 June 2019; Published 7 July 2019

Guest Editor: Zongli Xie

A more sustainable dialysis and water filtration membrane has been developed, by using the new, safer, bio-based solvent Cyrene® in place of N-methyl pyrrolidinone (NMP). The effects of solvent choice, solvent evaporation time, the temperature of casting gel, and coagulation bath together with the additive concentration on porosity and pore size distribution were studied. The results, combined with infrared spectra, SEM images, porosity results, water contact angle (WCA), and water permeation, confirm that Cyrene® is better media to produce polyethersulfone (PES) membranes. New methods, Mercury Intrusion Porosimetry (MIP) and NMR-based pore structure model, were applied to estimate the porosity and pore size distribution of the new membranes produced for the first time with Cyrene® and PVP as additive. Hansen Solubility Parameters in Practice (HSPiP) was used to predict polymer-solvent interactions. The use of Cyrene® resulted in reduced polyvinylpyrrolidone (PVP) loading than required when using NMP and gave materials with larger pores and overall porosity. Two different conditions of casting gel were applied in this study: a hot (70°C) and cold gel (17°C) were cast to obtain membranes with different morphologies and water filtration behaviours.

1. Introduction

The growing use of filtration membranes is the result of increasing attention paid to environmental problems linked to the availability of and growing demand for clean water [1–3]. Recent work has highlighted the need for new solvents in the membrane manufacturing process, in order to minimise the problems of toxic solvent release to the environment, with Polarclean®, DMSO Evol®, and ionic liquids being successfully applied in this process [4–8]. Porous polymeric membranes for water and wastewater treatment have traditionally been produced from cellulose acetate [9], polysulfone [10], polyvinylidene fluoride (PVDF) [11, 12], polyacrylonitrile (PAN) [13], and polyvinyl alcohol (PVA) [14]. Polyethersulfone (PES) is used in separation due to its excellent performance and high thermal, chemical, hydraulic, and mechanical stability. The polymer generates membranes ranging from nanofiltration (NF) and Reverse Osmosis (RO) used for desalinisation processes, to ultrafiltration (UF) used for food, metal, and textile industry and microfiltration (MF) for purification of beverages, and separation of oil and water emulsions. Fouling of the membrane is as a result of the hydrophobicity of PES, making separation unpredictable and shortening its lifetime due to a higher energy demand to push the water through the pores [15, 16]. To reduce the fouling effect, the PES membranes are modified *via* bulk modification, surface modification, and blending (a type of surface modification), with the latter being the most widely used method [17].

Filtration membranes have previously been fabricated using a casting solution of polyethersulfone (PES) in the repro-toxic solvents NMP [18–20], DMF [21], DMAc [22], or mixture of solvents [23, 24] along with a hydrophilic homopolymer, such as polyvinylpyrrolidone (PVP) [21, 24] or *poly*(ethylene glycol) (PEG) [25, 26], resulting in membranes less prone to fouling [25, 27]. DMSO has been utilised

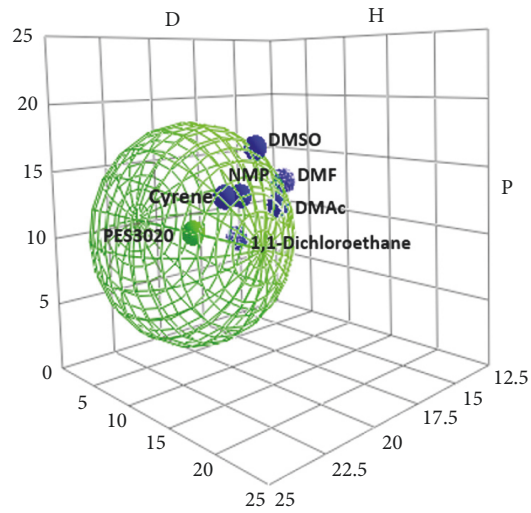

Figure 1: Recommended solvents mapped in Hansen space with solubility sphere for PES3020. Hansen solubility parameters are given here in units of $MPa^{1/2}$.

as the casting solvent [2, 28, 29], which is not in itself toxic, but it acts as a permeability enhancer and transfer compounds through the skin barrier. It is used in medicine as a skin adsorption enhancer for different drugs [30, 31]. Recently NMP was added to REACH's restricted substances list [32], due to the reproductive effects of this solvent. NMP and dichloromethane (DCM) were linked to foetal and adult deaths and their use has been banned or limited from paint stripping products by the big retailers. [33] DMF and DMAc are also on the Substances of Very High Concern (SVHC) list as toxic for reproduction (may damage the unborn child). The list of available and safe polar aprotic solvents is thus getting smaller.

The pore forming and structure controlling agents PVP and PEG are incorporated into PES matrix, similar to other polymer additives reported in the literature [20, 34, 35], so as to increase the hydrophilicity, diffusion properties (due to pore size distribution on the membrane surface) antifouling, and hemocompatibility properties of PES membranes [36–38]. These asymmetric membranes can be modified by adjusting any of the following factors: the composition of the casting solution (additives; solvent), the solvent evaporation temperature/time, and the method utilised. In this study we aim to substitute the traditional solvent used (NMP) with a greener, safer alternative. Cyrene® (dihydrolevoglucosenone) is a new commercially available, nontoxic solvent obtained from renewable waste and nonfood cellulosic source feedstock (e.g., straw, bagasse, and sawdust) (see Scheme 1). It is quickly proving to be a viable alternative polar aprotic solvent to both NMP and DMF [39–43].

Cyrene® is a polar aprotic solvent similar to NMP, but renewable, biodegradable, and nontoxic [39]. Cyrene® has been only given a hazard warning for being an eye irritant (E319) receiving an ECHA level 7 certification and has recently received permission to be sold in large quantities [44, 45]. Herein Cyrene® has been assessed for its suitability in substituting for NMP in the fabrication of PES membranes.

2. Materials and Methods

2.1. Materials. The flakes of Ultrason® E3020 P Polyarylethersulfone (Figure 2(4)) of 55,000 Da and a powder of PVP Luvitek® K-90 Pulver (Figure 2(5)) with 1,500,000 Da were obtained from INGE.BASF, Germany. The solvent Cyrene® was supplied by Circa Sustainable Chemicals Ltd., UK. All the other solvents used in this study were of reagent grade and purchased from Merck Co., UK, and VWR Chemicals ®, UK. Deionised water (DI) was provided in-house by the lab using an ELGA CENTRA® system. All chemicals were used without any further purification.

2.2. HSPiP's Predictive Power. Hansen Solubility Parameters (HSP) [46] were chosen to predict solubility of PES in different solvents by mapping the three values (dispersion interactions δD, dipolarity δP, and hydrogen bonding ability δH) in a three-dimensional "Hansen space", using 5th edition 5.0.03 of HSPiP (Hansen Solubility Parameters in Practice).

When determining whether a solvent will dissolve a sphere, it is useful to calculate the relative energy difference, *RED*:

$$RED = \frac{Ra}{Ro} \tag{1}$$

where *Ro* is the radius of interaction of a Hansen solubility parameter sphere determined experimentally (Figure 1) and *Ra* is the solubility parameter distance between polymer and solvent and can be calculated from

$$Ra^2 = 4\left(\delta D^{solvent} - \delta D^{solute}\right)^2 + \left(\delta P^{solvent} - \delta P^{solute}\right)^2 + \left(\delta H^{solvent} - \delta H^{solute}\right)^2 \tag{2}$$

A 3D representation (Figure 1) shows the distance of the solvents which dissolved the polymer and PES3020. A nonsolvent will have a *Ra* larger than the sphere's *Ro*, making

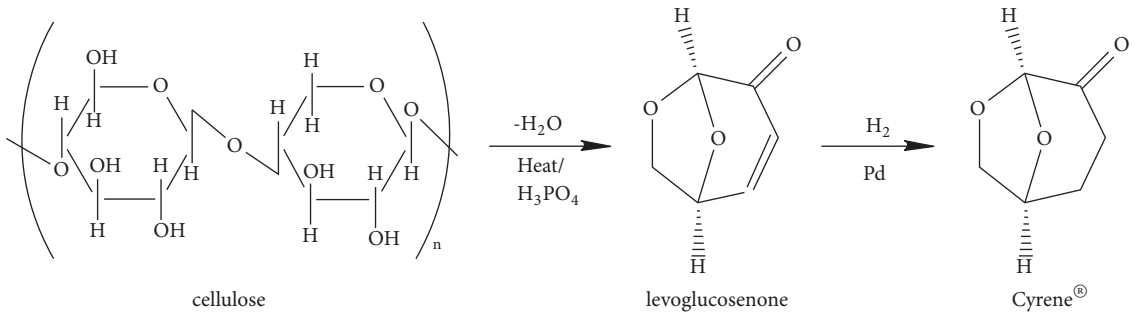

Scheme 1: Scheme of Cyrene® production from cellulose via levoglucosenone (LGO,).

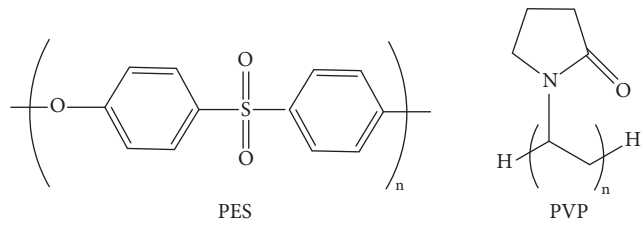

Figure 2: Chemical structure of PES and PVP.

RED > 1, while solvents likely to affect the material will have a RED < 1. A solvent with a RED < 1 and closer to the polymer's centre (with δD=20.42, δP=9.89, and δH=6.55) is predicted a better solvent. Cyrene® has the smallest distance from polymer in the Hansen space, suggesting the greatest affinity to PES3020 (Table 1). A full list of the solvents used can be found in the Supplementary Material accompanying the manuscript (SM Table 1).

As seen in Table 1, comparing HSP of Cyrene® and the other polar aprotic solvents, it was found that Cyrene® has a dispersion close to DMSO (18.9 *vs.* 18.4), a polarity parameter close to NMP (12.4 *vs.* 12.3), and a hydrogen bonding close to NMP (7.1 *vs.* 7.2). The similarity of Cyrene® to the other polar aprotic solvents has been studied previously [40].

2.3. Membrane Synthesis

2.3.1. Preparation of Casting Solutions. In this study, the polyethersulfone membranes (PES/C and PES/N) with highly asymmetrical pore structure were fabricated from hot (70°C) and cold (17°C) casting gels of PES, PVP, and solvent (Cyrene® or NMP), using a nonsolvent phase inversion technique (NIPS).

Table 2 shows the formulations of PES ultrafiltration flat sheet membranes using two different solvents and with/without PVP.

In this study, some of the characteristics of Cyrene® and NMP are presented in Table 3, showing the difference between the two solvents.

2.3.2. Membranes Fabrication. The casting solution was prepared by dissolving 20 wt% of PES pellets (as compared to the mass of solvent) into Cyrene® or NMP at a temperature of 70°C for 4h. Different concentrations of PVP were added under continuous stirring (Table 2). The casting solution was degassed and then placed on an acrylic plate for PES/N or on a Polyester (PET) nonwoven fabric CraneMat CU632 (Neenah Technical Materials, USA) for PES/C. The casting gel was cast using a RK Print K101 bench casting machine (RK Print, UK) at a speed of 3 cm s^{-1} for the membranes produced in NMP and 2 cm s^{-1} for membranes produced in Cyrene®. The speed of the casting machine was found to have a significant influence over membrane filtration and a slower speed was considered for PES/C due to its higher viscosity. The thickness of all membranes was controlled at 500 μm. The casting film was submerged in a coagulation bath containing deionised water at RT, causing the PES to precipitate. Membranes were then washed three times in distilled water for 10 minutes while under sonication in order to wash out residual solvent the fabricated membranes were then stored in deionised water until further use. The membranes were prepared at RT of 17°C and a humidity of 74-78%. The temperature of water bath was 12°C and the time from casting the gel to placing it in a water bath was limited to a maximum of 5 seconds.

Due to the higher density of Cyrene® and the amount of PVP used, both of which add to the total viscosity of the system; the gel was cast when hot. The viscosity of PES/C10 was tested using a Brookfield R/S plus Rheometer and shows a dramatic drop during the heating to 110°C (SM Figure 1), where its behaviour tends towards a Newtonian fluid.

2.4. Membrane Characterisation. To characterise the prepared membranes, they were first washed with deionised water and dried in vacuum oven at 80°C for 12 hours. The effects of the more viscous Cyrene® on the pore size, porosity, surface morphology, and mechanical properties of PES/PVP membranes were studied by scanning electron microscopy (SEM), pure water permeability, ATR-FTIR, and thermal analyses. FTIR and TGA reflected the physical or chemical

Table 1: Hansen Solubility Parameters [$MPa^{0.5}$] of different solvents and RED calculated for PES polymer.

Solvent	δD	δP	δH	Score	RED
Cyrene®	18.9	12.4	7.1	1	0.468
N-Methyl-2-Pyrrolidone	18	12.3	7.2	1	0.64
N,N-Dimethyl Acetamide	16.8	11.5	9.4	1	0.934
Dimethyl Sulfoxide	18.4	16.4	10.2	1	0.998
Dimethyl Formamide	17.4	13.7	11.3	1	1.008
1,1-Dichloroethane	16.5	7.8	3	1	1.041

Table 2: Composition of casting solutions (g).

Membrane type	Solution A			Solution B		
	PES	PVP	NMP	PES	PVP	Cyrene®
PES/0	16.7%	0%	83.3%	16.7%	0%	83.3%
PES/0.1	16.7%	0.08%	83.3%	16.7%	0.08%	83.3%
PES/0.5	16.6%	0.4%	83.0%	16.6%	0.4%	83.0%
PES/1	16.5%	0.8%	82.6%	16.5%	0.8%	82.6%
PES/5	16%	4%	80%	16%	4%	80%
PES/10	15.4%	7.7%	76.9%	15.4%	7.7%	76.9%

Table 3: Cyrene® and NMP safety data sheet.

Solvent	Empirical formula	Molecular weight (g mol^{-1})	Relative density (g mL^{-1} at 25°C)	B.P. (°C)	F.P. (°C)	M.P./F.P. (°C)
Cyrene®	$C_6H_8O_3$	128.13	1.25	227	108	-19.99
NMP	C_5H_9NO	99.13	1.028	202	91	-24

changes on the surface or in the bulk of PES membranes after modification.

ATR-FTIR spectra were recorded on a PerkinElmer Spectrum 400 FT-IR/FT-NIR Spectrometer with transmittance peaks in 4000-650 cm^{-1} region, with rapid scanning (4 scans) and resolution 4 cm^{-1} at room temperature.

Thermal stability of PES membranes was studied by TGA, giving weight loss of the produced membranes as a function of temperature. The membranes were heated from RT to 625°C at a rate of 10°C min^{-1} under a flow of nitrogen.

Scanning Electron Microscopy (SEM) images were taken on a JEOL JSM-6490LV, at 8kV from Bioscience Technology Facility, Biology Department, University of York, and were used to determine the morphology and structure of the membranes after they were frozen and fractured in liquid nitrogen followed by Au/Pd coating.

Porosity and pore size distribution test were determined using Mercury Intrusion Porosimetry (MIP) using a Micromeritics Autopore IV instrument located in the University of Leeds. This method is based on the behaviour of "nonwetting" liquids in capillary which cannot be absorbed by the pores of a solid itself, but requires an external pressure to be applied. By measuring the volume of mercury that intrudes into the sample material with each pressure change, the volume of pores in the corresponding size class can be obtained. MIP only shows accessible interconnected pores (if the closed pores are incompressible). The applied mercury pressure is inversely proportional to the size of the pores. A lower pressure is needed to penetrate large pores, while a greater pressure is needed to access smaller pores. From the pressure versus intrusion data, the instrument generates volume and size distributions using the Washburn equation:

$$D = \frac{-4\gamma \cos\theta}{P} \quad (3)$$

where D stands for pore diameter (μm), P is the applied pressure (psi), γ represents Hg-air surface tension (484 mN m^{-1}), and θ is Hg-air-porous material contact angle (140°).

NMR spectroscopy was used as supporting evidence of the pore size distributions and was considered a more sustainable and less toxic method compared to the MIP method, which can distort the skeletal porous structure of a sample [47]. However, this method was used previously to characterise porosity, pore geometry, connectivity, and permeability of sandstones and carbonates [48, 49]. In this project, the NMR was used to confirm the volume of fluid filling the pore space and a T2 distribution (equivalent to a pore size distribution, PSD) is obtained after deconvolution of magnetization relaxation (Figure 3).

As a measure of membrane's hydrophilicity, the water contact angle (WCA) was measured *via* the sessile drop method [50] using a Theta Lite optical tensiometer at a room temperature of 22°C. A range of 0.5–1.5 μL droplet sizes of water were placed on the membrane surface and the images were recorded using the automated OneAttension software. The static contact angles were measured at a minimum of three random locations and the mean values reported to minimise experimental error.

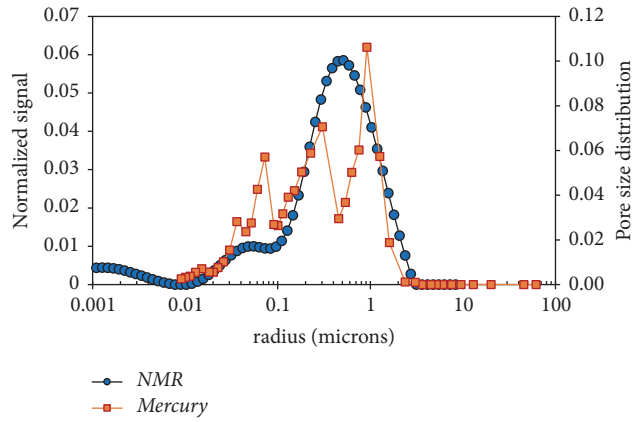

Figure 3: MIP and NMR methods of porosity using a PES/C5.

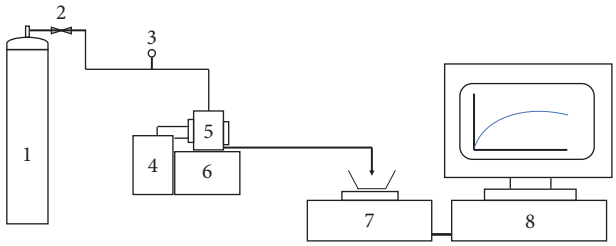

Figure 4: A schematic diagram of the frontal filtration equipment. (1) Nitrogen cylinder, (2) valve, (3) pressure sensor, (4) water bath, (5) membrane cell, (6) magnetic stirrer, (7) electronic balance, and (8) PC.

2.5. Pure Water Permeability Test. Membrane permeability was determined by measuring the pure water fluxes using a stirred cell (Sterlitech HP4750). The filtration solutions were stirred magnetically at 300 rpm and a constant temperature of 25± 0.5°C. Rates of filtration were determined by continuously weighing the filtrate on an electronic balance connected to a data logger. A digital electronic balance from Ohaus (Scout Pro Range), with an accuracy of 0.01 g was used to continuously measure the weight of the permeate. Recording the weight at certain time intervals also allows the calculation of the permeate flux:

$$Jw = \frac{m(t + \Delta t) - m(t)}{\rho A m \Delta t} \quad (4)$$

where J_w is the water flux (L m^{-2} h^{-1} (LMH)), m is the mass at a given time, ρ is the density of water, A_m is the area of the membrane (m^2), and t is the time (s).

Figure 4 shows schematically the arrangement of the membrane filtration and flux measurement equipment. The filtration cell was pressurised using nitrogen gas (oxygen free) with pressure controlled by means of a regulator on the cylinder. The 50 mm diameter membranes were first subject to an initial pressure of 1 bar until a stable flux was evident, then the pressure increased to 5 and 10 bar.

2.6. Gravimetric Method of Water Adsorption. This method is repeatedly used in literature to evaluate the porosity of the membranes[28, 50] *via* determining take up of water. The membranes were vacuum dried at 80°C, before being weighed and their size and thickness measured. They were then immersed in distilled water at RT for 24h, before being weighed again, and the increase in mass registered. The %water retained in pores was calculated using the following equation:

$$\varepsilon = \frac{\text{Ww} - \text{Wd}}{\text{Axlx}\rho}\text{x100} \quad (5)$$

where *Ww* and *Wd* represent wet and dry masses (g) of the membranes, respectively, *A* is the membrane surface area (m^2), *l* is thickness of membrane (m), and ρ is density of water at RT (998 Kg m^{-3}).

3. Results and Discussion

3.1. Porosity and Pore Size Distribution. The membranes are coded based on the solvent used (PES/C is the membrane produced with Cyrene® while PES/N represents the one with NMP) and the concentration of PVP used, *e.g.,* "0" means a membrane produced with no PVP, while "0.1" through to "10" means a membrane produced with 0.1% through to 10% PVP, respectively (Table 2). For example, a PES membrane produced with Cyrene® and 0.1% PVP will be referred to as "PES/C0.1" while the same membrane produced in NMP would be denoted "PES/N0.1".

As seen in Figure 5, the Cyrene-based membranes presented higher porosity in comparison to NMP in all cases, with a maximum of 79% and 78.8% for PES/C0.1 and PES/C1, respectively. The membrane prepared with Cyrene developed porosity even when not using pore forming PVP (PES/CO with 76.7% total porosity), which demonstrates superior porosity than a NMP-based membrane using pore forming additive (PES/N0.1) with 76.3% porosity. The membrane with 10% PVP has the lowest total porosity (54.9%), and at this point the membrane exhibits a different morphology (phenomenon seen in SEM images). On the other hand, the

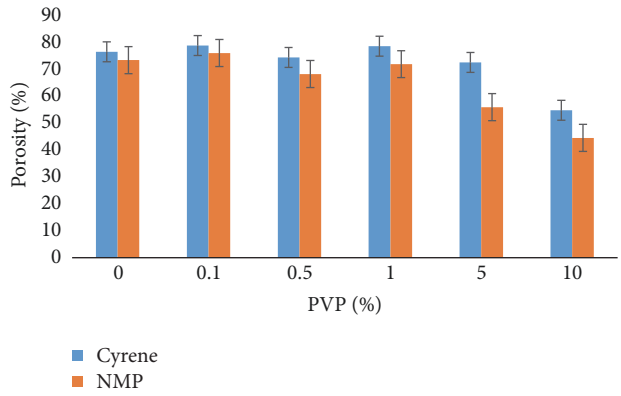

Figure 5: Overall porosity of the PES membranes prepared with Cyrene® (blue) and NMP (orange).

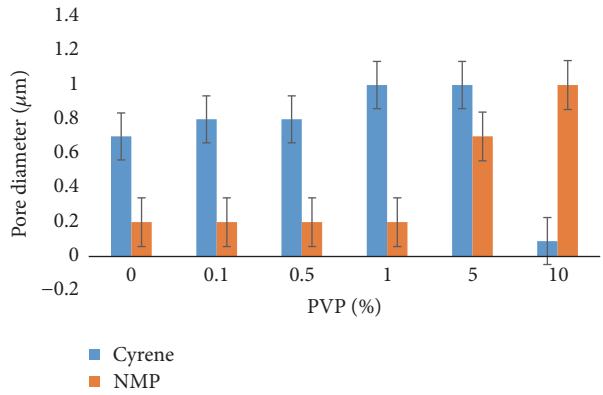

Figure 6: Overall pore diameters (μm) of PES/C (blue) and PES/N (orange).

highest porosity (76.3%), for the membranes produced with NMP is obtained with a PVP concentration of 0.1%. The lowest porosity for the membranes produced using NMP occurs for PES/N10 (44.6%).

It is also significant that 0.1% PVP is enough to produce good quality PES/C membranes, lowering the amount of sacrificial polymer represents an important starting point for the sustainable membrane fabrication together with substitution of a toxic petroleum-derived solvent with a safe, bio-based alternative.

Both Cyrene- and NMP-based membranes present a slightly decreasing porosity when 0.5% PVP is used (PES/C0.5 and PES/N0.5) and clearly decrease when using a higher concentration of PVP (PES/C5 and PES/N5). This decrease in porosity is more visible in the case of NMP-based membranes. However, this means that 1% of additive is clearly sufficient to give the maximum porosity in both types of membranes, with Cyrene-based membranes more superior than the NMP equivalents.

Figure 6 shows the pore diameter of membranes produced with Cyrene® and NMP. PES/C membranes developed bigger pores than PES/N, except for PES/C10, which has a different morphology. Interestingly, the pore size of a Cyrene-based membrane with no additive (PES/C0) has a similar pore diameter to that obtained in NMP-based membrane using at 5% PVP (PES/N5). This means that no additive is necessary to form pores when using Cyrene® as solvent. Similarly a membrane produced using Cyrene® and 1% PVP (PES/C1) shows the same pore diameter as a NMP-based membrane when using 10% (PES/N10) of the same pore forming agent. That means that less sacrificial pore forming agent is required when using Cyrene® as solvent compared to NMP-based systems.

Membranes prepared with Cyrene® have pore diameters from 0.09 μm (PES/C10) to 1 μm (PES/C1 and PES/C5), while the membranes prepared with NMP range between 0.2 μm (PES/N0, 0.1, 0.5, 1μm) to 1μm (PES/N10). Figure 6 clearly shows similarity between PES/C1 and PES/C5 to PES/N10 in pore size and pore distribution (SM Figure 2 and SM Figure 3). The membranes made using Cyrene® need 1% PVP to develop the biggest pores (PES/C1), while the membranes produced with NMP need twice as much PVP to develop the same pore diameter.

A high degree of variation in the pore system is seen when PVP concentration is increased. This is observed by the greater decrease in total porosity and an increase of pore diameters in the range between 0.5 and 1μm for PES/C0-5, followed by a dramatic decrease of pore diameter for PES/C10. The Cyrene-based membranes pore diameters follow a trend from a minimum with PES/C0 to a maximum

with PES/C5. Above a 5% PVP loading, this type of membranes drops drastically in pore diameter. This is as a result of the morphology of the membrane changing significantly, with large cavities containing very small pores on the walls (as clearly seen in Figure 10).

This morphology is clearly seen in PES/C10 where a 'diffusion membrane' has been formed, at which point it is believed that the pores of 0.09 μm are incorporated in the walls of cavities, replacing the classical macrovoids. The asymmetric membranes have variable pore diameters, from 0.001 to 10 μm while the symmetric one (PES/C10) present more uniform pores, with majority of pores of 1 μm diameter. PES/C0 presents a small quantity of pores of 0.1 μm; the quantity of this type of pores increases with increasing of PVP in casting solution and their presence is exclusively in PES/C10.

Membranes made using NMP increase their pore diameters with increasing PVP concentration from PES/N0-10. The NMP-based membranes present the same small pore diameter until a concentration of 5% of pore forming additive is added to the casting gel, leading to a bigger pore diameter with a maximum for PES/N10.

The results from NMR spectroscopy are consistent with the previously reported MICP results. The largest pores (around 10 μm) can be seen in the membranes produced with Cyrene®, increasing in line with the concentration of PVP used, with a maximum in PES/C5. For PES/N the number of larger pores increases with increasing PVP concentration, while smaller pores are no longer seen (*e.g.,* pores in the range 0.001 to 0.01 microns are only observed for PES/N0.1). After deconvolution of magnetization relaxation of Nuclear Magnetic Resonance (see Figure 7), the obtained T2 curves confirm the volume of fluid filling the pore space and indirectly the pore size distribution, described above by MICP method.

3.2. Membrane Characterisation

3.2.1. Membrane Functional Groups via FTIR Spectroscopy. The membranes present functional groups specific to PES, S=O symmetric stretch at 1149 cm^{-1}, C-SO_2-C asymmetric stretch at 1320 cm^{-1}, C-O asymmetric stretch at 1240 cm^{-1}, C_6H_6 ring stretch at 1578 and 1486 cm^{-1}, C-H stretch at 3096-3094 cm^{-1}, in addition to the residual PVP as indicated by a C=O stretch at 1667-1662 cm^{-1}, pyrrolidinyl radical at 1462 and 1423 cm^{-1}, C-N vibration at 1072 cm^{-1}, and C-H asymmetric stretch at 2950 cm^{-1}.

During the membrane precipitation step, some of the PES from the surface leaves the membrane together with most of the water-soluble polymer, but enough PVP remains (with its presence at 1667 cm^{-1} in Figure 8), providing the polymer surface with a more hydrophilic nature than the surface of PES alone.

In the case of PES/Cyrene®, coloration due to release of PES into the gelation media was less apparent than in the PES/NMP systems. This indicates a stronger PES/PVP interaction in Cyrene® (SM Figure 4).

3.2.2. Scanning Electron Microscopy (SEM) Analysis. All membranes produced herein (except for PES/C10) present a typical structure with a thin top layer supported on a sponge-like substructure (important for the mechanical resistance of the membranes), and macrovoids, due to the instantaneous demixing during the phase inversion [51], where PVP behaves as an antisolvent agent in the demixing step due to its high solubility in water. The casting solution has a high affinity for water which can cause changes in morphology and performance [4]. In this study the gel was cast and the glass plate with the casting gel was quickly immersed in the coagulation bath meaning the exposure to the atmosphere was less than 5 seconds. Finger-like structures can be seen near the inner (connecting the top layer to the sponge-like structure) and outer surface, while sponge structure can be seen in the centre of membranes. It has been generally accepted that instantaneous demixing leads to macrovoid structure and delayed demixing leads to a sponge-like structure [51, 52].

While the sponge-like structure looks the same in both Cyrene® and NMP producing membranes, Figure 9 shows the difference between them in a macrovoid layer at the same magnification.

When pure PES is used, the phase separation of polymer solution occurs immediately, due to low viscosity of the casting gel. The higher viscosity of Cyrene® (14.5 m Pa s at 20°C) compared to NMP (1.67 m Pa s at 20°C) adds to the casting gel's viscosity leading to a slower demixing process and hence to a more visible sponge-like structure (Figure 10). The modification of polymer solution (by adding PVP) changes the pore structure of the membrane [53]. Also, different temperatures of the casting gel lead to differences in their morphology (Figure 10):

The membranes cast from the cold gels present more finger-like layers than the plain PES/C0 (which is more viscous), especially in the middle of the membrane. The membranes cast from Cyrene® hot gels showed more sponge-like structure, with macrovoids all the way through the membrane. A greater difference in morphology starts from a concentration of 5% PVP, with the greatest at a concentration of 10% PVP. PES/C10 from a hot gel (Figure 10(l)) developed a completely different surface morphology, a symmetrical-like structure, looking like a porous web or sponge. This could be caused by the large amount of PVP which slowed precipitation. When cast from a cold gel, the membrane shows asymmetrical layers with bigger space (Figure 10(i)). Increasing the PVP content in the casting solution led to slower demixing, especially towards the bottom layer of membrane (closest to the glass slide). When the exchange from solvent to antisolvent occurs, it starts at the surface, where finger voids are observed and slows as it approaches the bottom layer, when more sponge-like structures are seen. This structure presents pores which increase in diameter from the top to the bottom surface of the membrane. The rheology of the casting gel of PES/C10 was studied, with a decrease in viscosity with increasing temperature clearly visible (SM Figure 1). This had a great impact on the membrane morphology and differences in the permeability data are expected. A clear difference between the membranes cast from hot/cold gels is seen in NMP's case too (red circle

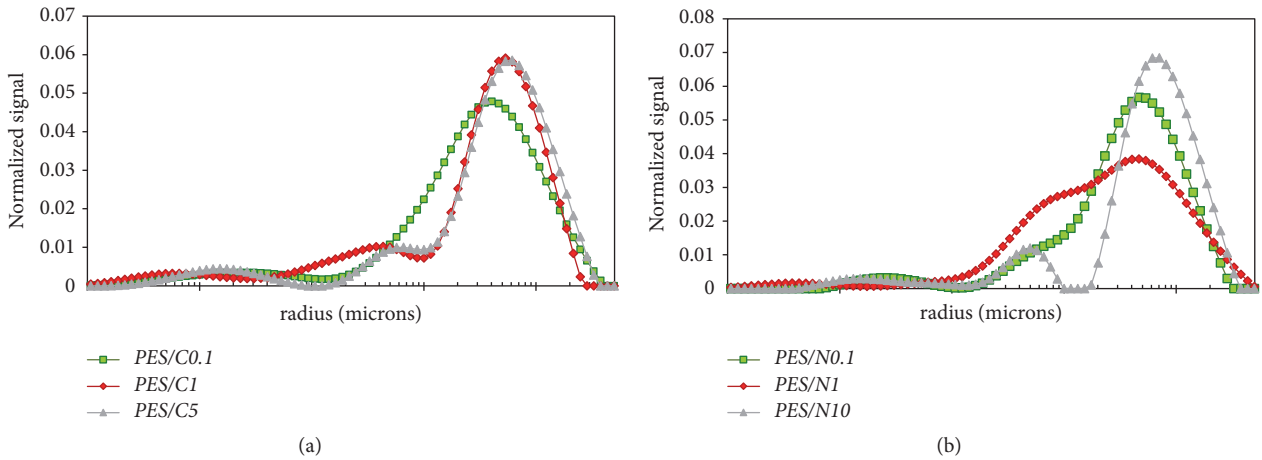

Figure 7: Pore size distribution of PES produced with Cyrene® (a) and NMP (b) using NMR.

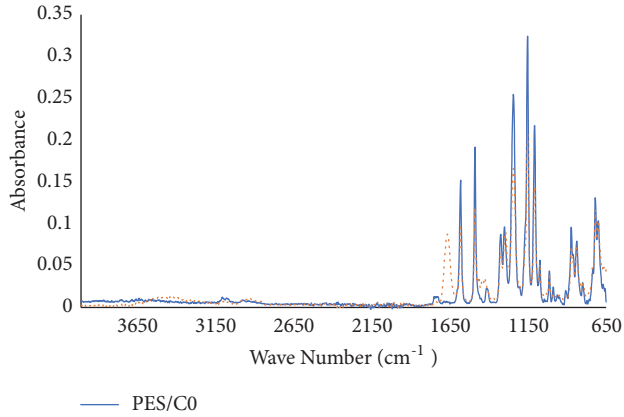

Figure 8: Fourier transform infrared spectrum of PES/C.

in SM Figure 5) where the one cast from a hot gel presents a middle sponge layer, while the one cast from a cold gel clearly shows the finger layer all the way through the membrane.

3.2.3. Thermal Stability of Membranes. The results of thermogravimetric analysis on the membranes prepared here are shown in Figure 11 and Table 4. PVP has a decomposition temperature around 440°C, while PES3020 decomposes at 580-600°C, which means that PVP would lose more weight before PES began to decompose.

The first degradation took place below 120°C due to moisture loss, followed by Cyrene® volatilisation at around 170°C and 140°C for NMP, followed by PVP decomposition at *ca.* 420°C and PES decomposition at *ca.* 580-600°C. The differential thermogravimetric data shows a greater amount of residual PVP from PES/C membranes.

PES/C membranes consistently show a higher thermal stability than PES/N equivalents. PES/C0 has a thermal decomposition of 588.7°C, while PES/N0 decomposes at 578.4°C, which means that a greater energy is required to break the bonds of PES/C membrane. The peak of the 1st derivative (inflection point) indicates the point of greatest rate of change on the weight loss curve, as seen in Figures 11(b) and 11(d).

The addition of PVP to the membranes decreases the thermal stability, due to a lower decomposition temperature of PVP than of PES, but the miscibility of both polymers was confirmed from the thermal analysis. The differences between the concentration of PVP and TGA residue may be due to PVP remaining in the membranes after washing with water, depending on the membranes porosity and pore size. It was found that PES/N membranes lose some PES from the membrane surface when casting the film. The same membranes lost more PES and PVP than PES/C, which means that Cyrene® makes a better media for this type of filtration as well as being more hydrophilic.

3.3. Surface Wetting Property of the New Membranes Produced with Cyrene®. As shown in Figure 12(a), the static water contact angle of the new PES films produced with Cyrene® decreased from 73.1% for PES/C0 to 37.5% for PES/C10, with a hydrophilic character in all cases. This decreasing of the contact angle indicates increasing in hydrophilicity of these membranes with increasing residual PVP content.

The wetting changes were recorded over time by means of the same methodology used for static contact angle, but with values taken over a 300 second range. It can be seen in Figure 12(b) how the droplets change in a reproducible

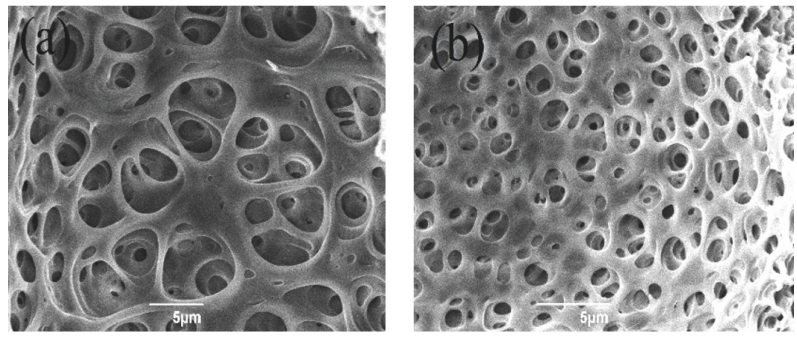

(a) (b)

Figure 9: SEM images of PES/C0.1 (a) and PES/N0.1 (b) in detail.

Table 4: Thermogravimetric (TGA) analysis measurements of PES/C and PES/N membranes.

C/Sample	Residue%	Tm (°C)	N/Sample	Residue	Tm (°C)
PES3020	38	589.7			
PVP K90	5.3	443.2			
PES/C0	30.6	588.7	PES/N0	30.4	572.9
PES/C0.1	32.3	577.2	PES/N0.1	24.1	564.8
PES/C0.5	30.2	588.5	PES/N0.5	25.3	569.2
PES/C1	30.2	580.5	PES/N1	30.5	576.2
PES/C5	41.9	568.2	PES/N5	23.5	546.7
PES/C10	39.8	580.7	PES/N10	22.8	561.7

manner and reduce their contact angle. A larger initial drop occurs as water rapidly fills pores at the surface of the membrane, until locally saturated. This phenomenon was found to be due to a result of the advancing angle (higher angle which relies on the hydrophobic surface component) changing into a receding angle (low contact angle of the hydrophilic component) upon a decrease in droplet volume and is due to imbibition and evaporation. [54]

The contact angle of PES/C0 recorded the smallest change during the test time, due to a less hydrophilic character and the tendency of the droplet to be repulsed by the membrane surface at least at the beginning. Over the time, when the membrane is locally saturated, the droplet moves into the porous membrane and the contact angle changes. On the other side, PES/C10 membrane was found to have the most dramatic change in its contact angle, due to the most hydrophilic character and its porosity. The SEM images of the PES/C10 demonstrated a very porous membrane which would allow the droplet of water to be completely absorbed in under 60 seconds during the WCA experiment.

3.4. Pure Water Permeability. Pure water permeability (PWP) testing was evaluated based on water flux. Evidence in the literature indicates that the sponge layer filters are slower than the finger layer of a membrane [51].

Based on these criteria, the permeate flux seen in Figure 13 shows differences between the membranes depending on the solvent used, the concentration of PVP used, and temperature of the casting gel. The membranes produced using Cyrene® and cast from a cold gel show an increasing permeability when PVP is added with a maximum at 10% PVP, but with no permeability when using 0.5, 1, and 5% PVP. This is explained by the morphology of the membrane, with more finger layers on top of the membrane a dense sponge layer at the bottom of the membrane. This is due to the thickness of membrane chosen in this project (500 μm) which results in different morphologies most likely depending on speed of exchange between the solvent and water (SM Figure 6). At the top surface, this is rapid, with the polymer precipitating out and voids forming as a result of water displacement. At the bottom, crystallisation has dominated, with fewer voids. This results in low permeability as the finger regions are not interconnected. The concentration of PVP used had a great impact of permeability when using over 0.1% PVP, when the produced membranes showed no flux, due to the presence of dead ends of the finger layers presented in their morphologies. The new membranes PES/C0 and PES/C0.1 cast from cold gels together with PES/C0 from a hot gel are believed to be suitable for a ultrafiltration (UF), while a permeability is lower than 20 LMH/bar for a nanofiltration/reverse osmosis (NF/RO), while the PES/C10 membrane showed greater fluxes more in keeping of a microfiltration membrane (MF). Instead, when the same membranes are cast from a hot gel, the produced membranes showed a permeability with a maximum at 10% PVP, but with a smaller permeate flux than the corresponding cold gel membrane. The membranes produced from a cold gel, using Cyrene® and a PVP concentration above 0.1%, developed a morphology

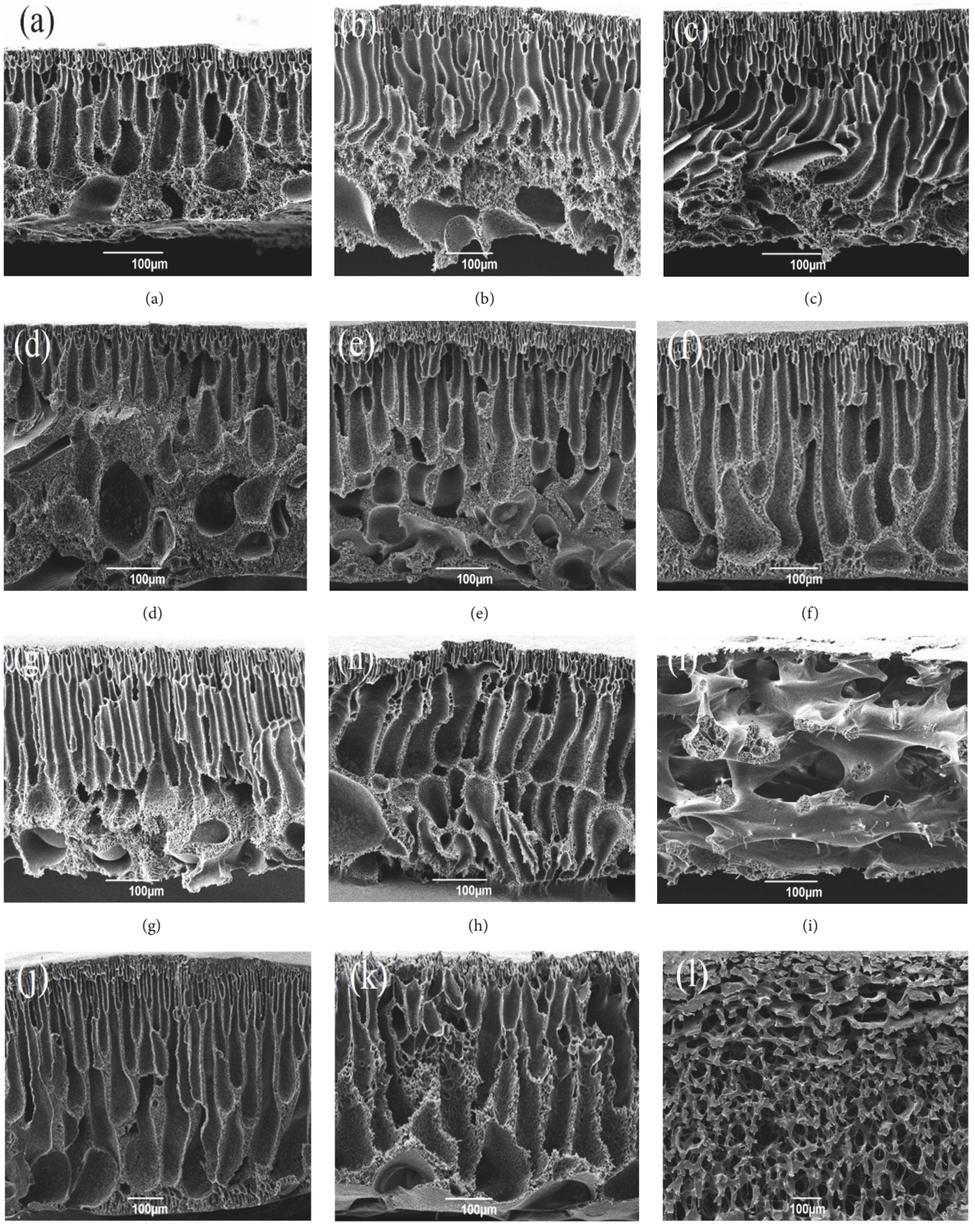

Figure 10: SEM cross-section of membranes produced from Cyrene and different concentrations of PVP: 0% (a, d), 0.1% (b, e), 0.5% (c, f), 1% (g, j), 5% (h, k), and 10% (i, l) in cold (first letter) and hot gels (second letter).

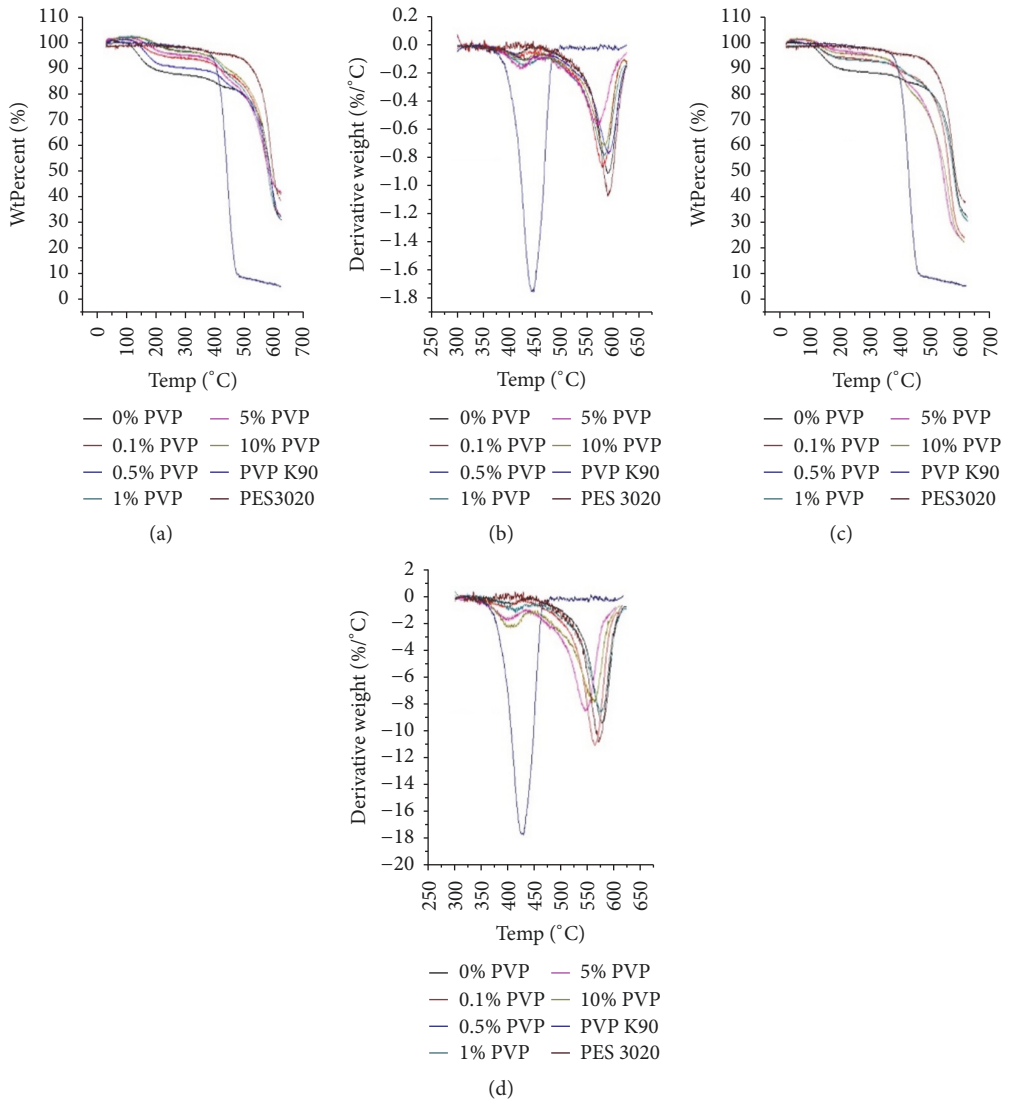

Figure 11: TGA and DTG spectra of PES/C (a-b) and PES/N membranes (c-d). Note: TGA, thermogravimetric analysis; DTG, differential thermogravimetric.

with finger layers in the middle of the membrane but are not interconnected to the surface, thus registering no permeate flux.

When adding PVP, the permeability also increased in PES/N, with a maximum flux at 10% PVP and when the membrane was cast from a cold gel. When cast from a hot gel, the membrane produced from the same concentration of PVP showed a higher flux of water due to a void in the middle of the membrane which permitted a higher permeability. Looking at Figures SM 5(b) and 5(e) relating to 0.1N, the hot cast seems to have a layer in which all the pores appear blocked about 1/2 way through the membrane (red circle in SM Figure 5(e)). However, in the cold cast, the pores appear to traverse the membrane (red circle in SM Figure 5(b)). The presence of the middle sponge layer in PES/N membranes which were hot cast showed a lower permeability than the ones coming from a cold gel, except for PES/N0.5, where the morphology shows a thicker sponge layer, which would generally slow the flux down.

3.5. Gravimetric Analysis. Figure 14 shows the absorption capacity of PES/C (in blue) and PES/N (in orange) to retain pure water in their pores. Although less precise than other methodologies applied in this research, this is the standard test to evaluate membrane porosity [17].

Figure 14 shows that PES/C consistently developed a greater water retention capacity than the respective PES/N membrane (consistent with MICP and SEM data). MICP and gravimetric data present differences between the samples generated using the same solvent. For example, gravimetrically PES/C5 presents the biggest capacity of water absorption, while for MICP data, PES/C0.1 has the biggest total

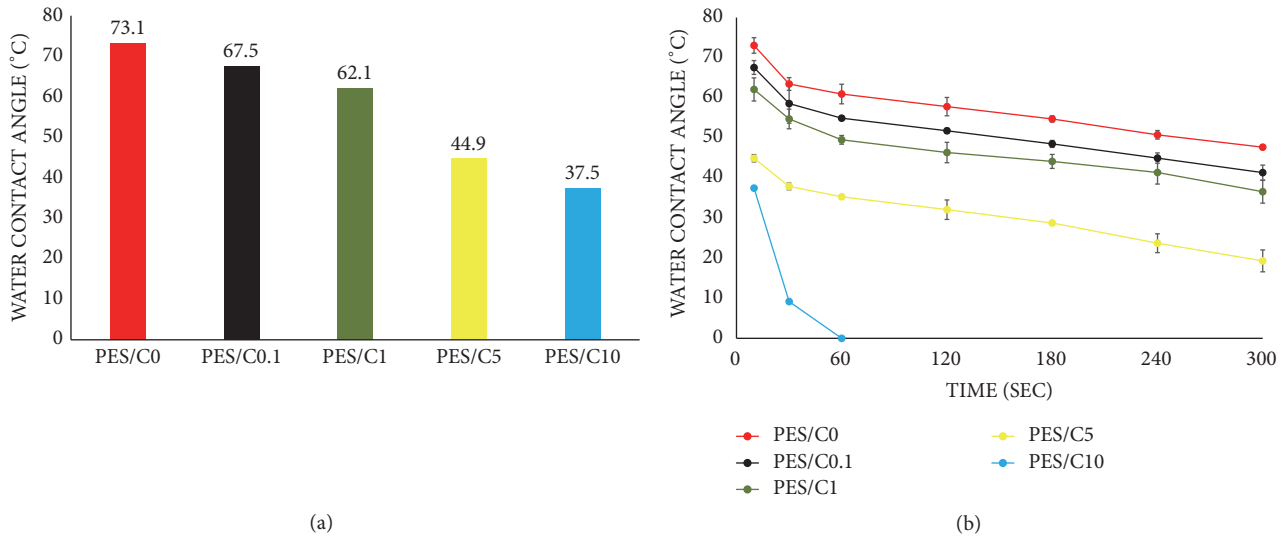

Figure 12: The static water contact angle (a) and the time-depended values (b) for a sessile drop spreading over a range of PES membranes produced with Cyrene®.

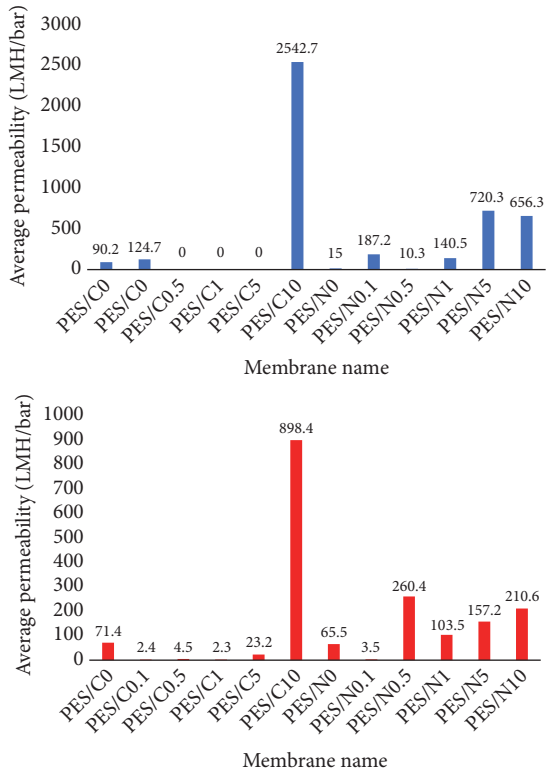

Figure 13: Pure water permeability of membranes cast from cold (in blue) and hot (in red) gel.

porosity. However, PES/C10 showed the smallest capacity to retain water, which is entirely consistent with MICP and SEM data.

4. Conclusions

Polyethersulfone flat sheet membranes for water filtration applications were prepared by the NIPS technique employing Cyrene® as an alternative solvent and compared to PES produced using the traditional NMP. Membrane morphology and performance were tailored acting on the casting solution composition and temperature. The new membranes produced with Cyrene® are more sustainable, with less of both polymers' loss and tunable pore size and contact angles, from a less hydrophilic PES/C0 to a more hydrophilic PES/C10 when the hydrophilic additive is added to the

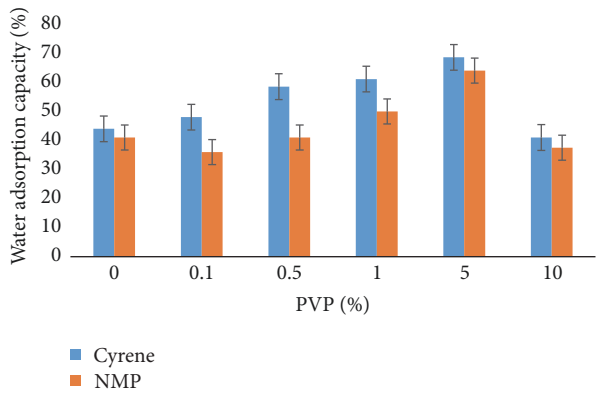

Figure 14: Gravimetric analysis of PES/C and PES/N.

casting solution. The produced membranes with the bio-based solvent Cyrene® showed a greater total porosity, bigger pore size, and higher thermal stability, compared to the PES membranes produced with NMP. It was found that no additive is necessary to form pores when Cyrene® is applied as solvent, PES/C0 having the same pore diameter as NMP-based membranes produced with 5% PVP (PES/N5), meaning that no additive many not be necessary for the role of pore forming when using Cyrene®. PES membranes produced with Cyrene® and 0.1% PVP (PES/C0.1) and 1% PVP (PES/C1) developed the largest porosity (ca. 79%) for the both Cyrene® and NMP-based membranes. PES produced with Cyrene® and minimal concentration of PVP (0.1% PVP) developed the same pore diameter as PES produced with NMP at a higher concentration of PVP (5%) and the largest pores are registered in PES when using Cyrene® with 1% PVP, while for a membrane produced with NMP, the largest pore diameter appears using a higher concentration of PVP (10%). The permeability of the new membranes produced with Cyrene® was easily tailored in the range between NF/RO to MF, by changing the temperature of the casting gel, whereas only slightly small changes were observed when using NMP. While the PES/N showed a trend with a maximum filtration for PES/N cast from a cold gel when 5% PVP was used, the same membranes cast from a hot gel showed no supporting trend, probably because NMP evaporated quicker than Cyrene at elevated temperatures. Completely new morphologies were found in PES produced in Cyrene®, when using 10% PVP, regardless if cast hot or cold. When using Cyrene, the morphology was different for the two casting gels, with a symmetrical one observed when hot cast; this is less obvious when cast from a cold gel. Both hot and a cold cast PES/C10 have showed the best filtrate flux, with the potential, for application in microfiltration. Utilising cold casting, minimal addition of PVP leads to better filtration properties than the corresponding membrane produced without any additive; this suggests PES/C0.1 has applications as a hydrophilic, highly biocompatible/haemodialysis ultrafiltration membrane. The relatively high viscosity of Cyrene® adds to the overall viscosity of the PES/PVP casting gel and this can be exploited to tailor membranes to different ranges of filtration with different physical properties. Decreasing viscosity with temperature is a potential factor to consider when casting membranes containing Cyrene®.

Data Availability

Data supporting this publication is available in the supporting information while additional raw data is available via https://doi.org/10.15124/c6545fa3-c5aa-4741-9ad0-1fe092f292cf.

Conflicts of Interest

The authors declare that they have no conflicts of interest.

Acknowledgments

We extend our thanks to INGE.BASF for providing PES and PVP polymers used in this project, Meg Stark from Bioscience Technology Facility, Biology Department, University of York for SEM images, and Dr Carlos Grattoni from School of Earth and Environment, Leeds University for mercury porosimetry and low-field NMR spectroscopy. The authors would like to acknowledge Circa Sustainable Chemicals Ltd. for its financial support of this work.

Supplementary Materials

Supplementary information is available and contains a table listing all the solvents studied via HSPiP (SM Table 1); a plot for the temperature dependent viscosity of the PES/C10 sample over the range of room temperature to 110°C (SM Figure 1); MICP pore diameter distributions for each sample prepared in Cyrene® (SM Figure 2) or NMP (SM Figure 3); a photograph showing the coagulation bath of PES/PVP membranes in Cyrene® and NMP (SM Figure 4); SME cross-section images of each membrane prepared in NMP (SM Figure 5); SEM cross-section images of PES/C1 at different thickness (SM Figure 6). *(Supplementary Materials)*

References

[1] S. Al Aani, C. J. Wright, and N. Hilal, "Investigation of UF membranes fouling and potentials as pre-treatment step in desalination and surface water applications," *Desalination*, vol. 432, pp. 115–127, 2018.

[2] Y. L. Thuyavan, N. Anantharaman, G. Arthanareeswaran, and A. F. Ismail, "Impact of solvents and process conditions on the formation of polyethersulfone membranes and its fouling behavior in lake water filtration," *Journal of Chemical Technology and Biotechnology*, vol. 91, no. 10, pp. 2568–2581, 2016.

[3] M. Omidvar, M. Soltanieh, S. M. Mousavi, E. Saljoughi, A. Moarefian, and H. Saffaran, "Preparation of hydrophilic nanofiltration membranes for removal of pharmaceuticals from water," *Journal of Environmental Health Science and Engineering*, vol. 13, no. 1, 2015.

[4] T. Marino, E. Blasi, S. Tornaghi, E. Di Nicolò, and A. Figoli, "Polyethersulfone membranes prepared with Rhodiasolv®Polarclean as water soluble green solvent," *Journal of Membrane Science*, vol. 549, pp. 192–204, 2018.

[5] D. S. Lakshmi, T. Cundari, E. Furia et al., "Preparation of Polymeric Membranes and Microcapsules Using an Ionic Liquid as Morphology Control Additive," *Macromolecular Symposia*, vol. 357, no. 1, pp. 159–167, 2015.

[6] D. Kim, O. R. Salazar, and S. P. Nunes, "Membrane manufacture for peptide separation," *Green Chemistry*, vol. 18, no. 19, pp. 5151–5159, 2016.

[7] D. Kim, H. Vovusha, U. Schwingenschlögl, and S. P. Nunes, "Polyethersulfone flat sheet and hollow fiber membranes from solutions in ionic liquids," *Journal of Membrane Science*, vol. 539, pp. 161–171, 2017.

[8] T. Marino, F. Galiano, S. Simone, and A. Figoli, "DMSO EVOL™ as novel non-toxic solvent for polyethersulfone membrane preparation," *Environmental Science and Pollution Research*, vol. 26, no. 15, pp. 14774–14785, 2019.

[9] M. Elimelech, . Xiaohua Zhu, A. E. Childress, and . Seungkwan Hong, "Role of membrane surface morphology in colloidal fouling of cellulose acetate and composite aromatic polyamide reverse osmosis membranes," *Journal of Membrane Science*, vol. 127, no. 1, pp. 101–109, 1997.

[10] K. Kim, K. Lee, K. Cho, and C. Park, "Surface modification of polysulfone ultrafiltration membrane by oxygen plasma treatment," *Journal of Membrane Science*, vol. 199, no. 1-2, pp. 135–145, 2002.

[11] Z. Wang, H. Yu, J. Xia et al., "Novel GO-blended PVDF ultrafiltration membranes," *Desalination*, vol. 299, pp. 50–54, 2012.

[12] S. Ayyaru and Y. Ahn, "Application of sulfonic acid group functionalized graphene oxide to improve hydrophilicity, permeability, and antifouling of PVDF nanocomposite ultrafiltration membranes," *Journal of Membrane Science*, vol. 525, pp. 210–219, 2017.

[13] I. Sentana, M. De La Rubia, M. Rodríguez, E. Sentana, and D. Prats, "Removal of natural organic matter by cationic and anionic polyacrylonitrile membranes. The effect of pressure, ionic strength and pH," *Separation and Purification Technology*, vol. 68, no. 3, pp. 305–311, 2009.

[14] E. Yang, X. Qin, and S. Wang, "Electrospun crosslinked polyvinyl alcohol membrane," *Materials Letters*, vol. 62, no. 20, pp. 3555–3557, 2008.

[15] M. KOH, M. CLARK, and K. HOWE, "Filtration of lake natural organic matter: Adsorption capacity of a polypropylene microfilter," *Journal of Membrane Science*, 2005.

[16] X. Ma, Y. Su, Q. Sun, Y. Wang, and Z. Jiang, "Enhancing the antifouling property of polyethersulfone ultrafiltration membranes through surface adsorption-crosslinking of poly(vinyl alcohol)," *Journal of Membrane Science*, vol. 300, no. 1-2, pp. 71–78, 2007.

[17] C. Zhao, J. Xue, F. Ran, and S. Sun, "Modification of polyethersulfone membranes—a review of methods," *Progress in Materials Science*, vol. 58, no. 1, pp. 76–150, 2013.

[18] N. Maximous, G. Nakhla, and W. Wan, "Preparation, characterization and performance of Al_2O_3/PES membrane for wastewater filtration," *Journal of Membrane Science*, vol. 341, no. 1, pp. 67–75, 2009.

[19] R. Boom, T. van den Boomgaard, and C. Smolders, "Mass transfer and thermodynamics during immersion precipitation for a two-polymer system," *Journal of Membrane Science*, vol. 90, no. 3, pp. 231–249, 1994.

[20] J.-H. Kim and K.-H. Lee, "Effect of PEG additive on membrane formation by phase inversion," *Journal of Membrane Science*, vol. 138, no. 2, pp. 153–163, 1998.

[21] S. Zhao, W. Yan, M. Shi, Z. Wang, J. Wang, and S. Wang, "Improving permeability and antifouling performance of polyethersulfone ultrafiltration membrane by incorporation of ZnO-DMF dispersion containing nano-ZnO and polyvinylpyrrolidone," *Journal of Membrane Science*, vol. 478, pp. 105–116, 2015.

[22] M. Khorsand-Ghayeni, J. Barzin, M. Zandi, and M. Kowsari, "Fabrication of asymmetric and symmetric membranes based on PES/PEG/DMAc," *Polymer Bulletin*, vol. 74, no. 6, pp. 2081–2097, 2017.

[23] K. Yoon, B. S. Hsiao, and B. Chu, "Formation of functional polyethersulfone electrospun membrane for water purification by mixed solvent and oxidation processes," *Polymer Journal*, vol. 50, no. 13, pp. 2893–2899, 2009.

[24] A. Rahimpour and S. Madaeni, "Polyethersulfone (PES)/cellulose acetate phthalate (CAP) blend ultrafiltration membranes: Preparation, morphology, performance and antifouling properties," *Journal of Membrane Science*, vol. 305, no. 1-2, pp. 299–312, 2007.

[25] A. Idris, N. Mat Zain, and M. Noordin, "Synthesis, characterization and performance of asymmetric polyethersulfone (PES) ultrafiltration membranes with polyethylene glycol of different molecular weights as additives," *Desalination*, vol. 207, no. 1-3, pp. 324–339, 2007.

[26] B. Chakrabarty, A. K. Ghoshal, and M. K. Purkait, "Effect of molecular weight of PEG on membrane morphology and transport properties," *Journal of Membrane Science*, vol. 309, no. 1-2, pp. 209–221, 2008.

[27] H. Qin, S. Nie, C. Cheng et al., "Insights into the surface property and blood compatibility of polyethersulfone/polyvinylpyrrolidone composite membranes: toward high-performance hemodialyzer," *Polymers for Advanced Technologies*, vol. 25, no. 8, pp. 851–860, 2014.

[28] I. Sadeghi, A. Aroujalian, A. Raisi, B. Dabir, and M. Fathizadeh, "Surface modification of polyethersulfone ultrafiltration membranes by corona air plasma for separation of oil/water emulsions," *Journal of Membrane Science*, vol. 430, pp. 24–36, 2013.

[29] G. Arthanareeswaran and V. M. Starov, "Effect of solvents on performance of polyethersulfone ultrafiltration membranes: Investigation of metal ion separations," *Desalination*, vol. 267, no. 1, pp. 57–63, 2011.

[30] P. Karande and S. Mitragotri, "Enhancement of transdermal drug delivery via synergistic action of chemicals," *Biochimica*

et Biophysica Acta (BBA) - Biomembranes, vol. 1788, no. 11, pp. 2362–2373, 2009.

[31] H. Marwah, T. Garg, A. K. Goyal, and G. Rath, "Permeation enhancer strategies in transdermal drug delivery," *Drug Delivery*, vol. 23, no. 2, pp. 564–578, 2014.

[32] "1-methyl-2-pyrrolidone - Substances restricted under REACH - ECHA, (n.d.)," https://echa.europa.eu/substances-restricted-under-reach/-/dislist/details/0b0236e1827f617f, 2018.

[33] "Regulations.gov - Docket Folder Summary, (n.d.)," https://www.regulations.gov/docket?D=EPA-HQ-OPPT-2016-0231, 2018.

[34] R. Boom, I. Wienk, T. van den Boomgaard, and C. Smolders, "Microstructures in phase inversion membranes. Part 2. The role of a polymeric additive," *Journal of Membrane Science*, vol. 73, no. 2-3, pp. 277–292, 1992.

[35] D. Mosqueda-Jimenez, R. Narbaitz, T. Matsuura, G. Chowdhury, G. Pleizier, and J. Santerre, "Influence of processing conditions on the properties of ultrafiltration membranes," *Journal of Membrane Science*, vol. 231, no. 1-2, pp. 209–224, 2004.

[36] F. Ran, S. Nie, Z. Yin et al., "Synthesized negatively charged macromolecules (NCMs) for the surface modification of anticoagulant membrane biomaterials," *International Journal of Biological Macromolecules*, vol. 55, pp. 269–275, 2013.

[37] S. Zinadini, A. A. Zinatizadeh, M. Rahimi, V. Vatanpour, and H. Zangeneh, "Preparation of a novel antifouling mixed matrix PES membrane by embedding graphene oxide nanoplates," *Journal of Membrane Science*, vol. 453, pp. 292–301, 2014.

[38] Z. Yi, L. Zhu, Y. Xu, Y. Zhao, X. Ma, and B. Zhu, "Polysulfone-based amphiphilic polymer for hydrophilicity and fouling-resistant modification of polyethersulfone membranes," *Journal of Membrane Science*, vol. 365, no. 1-2, pp. 25–33, 2010.

[39] D. E. Richardson and W. D. Raverty, "Predicted environmental effects from liquid emissions in the manufacture of levoglucosenone and Cyrene TM," *Appita Journal*, vol. 69, no. 4, pp. 344–351, 2016.

[40] J. Sherwood, M. De bruyn, A. Constantinou et al., "Dihydrolevoglucosenone (Cyrene) as a bio-based alternative for dipolar aprotic solvents," *Chem. Commun.*, vol. 50, no. 68, pp. 9650–9652, 2014.

[41] H. J. Salavagione, J. Sherwood, M. De bruyn et al., "Identification of high performance solvents for the sustainable processing of graphene," *Green Chemistry*, vol. 19, no. 11, pp. 2550–2560, 2017.

[42] J. Zhang, G. B. White, M. D. Ryan, A. J. Hunt, and M. J. Katz, " Dihydrolevoglucosenone (Cyrene) As a Green Alternative to *N,N* -Dimethylformamide (DMF) in MOF Synthesis ," *ACS Sustainable Chemistry & Engineering*, vol. 4, no. 12, pp. 7186–7192, 2016.

[43] L. Mistry, K. Mapesa, T. W. Bousfield, and J. E. Camp, "Synthesis of ureas in the bio-alternative solvent Cyrene," *Green Chemistry*, vol. 19, no. 9, pp. 2123–2128, 2017.

[44] "(1S,5R)-6,8-dioxabicyclo[3.2.1]octan-4-one - Substance Information - ECHA," https://echa.europa.eu/substance-information/-/substanceinfo/100.234.612.

[45] "Press Release: Circa Receives Green Light to Sell Non-toxic, Bio-based and Biodegradable Solvent in EU, (n.d.)," https://www.sustainabilityconsult.com/news/361-press-release-circa-receives-green-light-to-sell-non-toxic-bio-based-and-biodegradable-solvent-in-eu, 2018.

[46] C. M. Hansen, "The Universality of the Solubility Parameter," *Industrial & Engineering Chemistry Product Research and Development*, vol. 8, no. 1, pp. 2–11, 1969.

[47] P. A. Gane, C. J. Ridgway, E. Lehtinen et al., "Comparison of NMR Cryoporometry, Mercury Intrusion Porosimetry, and DSC Thermoporosimetry in Characterizing Pore Size Distributions of Compressed Finely Ground Calcium Carbonate Structures," *Industrial & Engineering Chemistry Research*, vol. 43, no. 24, pp. 7920–7927, 2004.

[48] Y. Yao, D. Liu, Y. Che, D. Tang, S. Tang, and W. Huang, "Petrophysical characterization of coals by low-field nuclear magnetic resonance (NMR)," *Fuel*, vol. 89, no. 7, pp. 1371–1380, 2010.

[49] E. Suuberg, "Elastic behaviour of coals studied by mercury porosimetry," *Fuel*, vol. 74, no. 10, pp. 1522–1530, 1995.

[50] M. Peydayesh, M. Bagheri, T. Mohammadi, and O. Bakhtiari, "Fabrication optimization of polyethersulfone (PES)/polyvinylpyrrolidone (PVP) nanofiltration membranes using Box–Behnken response surface method," *RSC Advances*, vol. 7, no. 40, pp. 24995–25008, 2017.

[51] H. Strathmann, K. Kock, P. Amar, and R. Baker, "The formation mechanism of asymmetric membranes," *Desalination*, vol. 16, no. 2, pp. 179–203, 1975.

[52] E. Saljoughi, M. Amirilargani, and T. Mohammadi, "Effect of poly(vinyl pyrrolidone) concentration and coagulation bath temperature on the morphology, permeability, and thermal stability of asymmetric cellulose acetate membranes," *Journal of Applied Polymer Science*, vol. 111, no. 5, pp. 2537–2544, 2009.

[53] N. Arahman, T. Maimun, Mukramah, and Syawaliah, "The study of membrane formation via phase inversion method by cloud point and light scattering experiment," in *Proceedings of the AIP Conf*, 2017.

[54] T. H. Muster and C. A. Prestidge, "Application of time-dependent sessile drop contact angles on compacts to characterise the surface energetics of sulfathiazole crystals," *International Journal of Pharmaceutics*, vol. 234, no. 1-2, pp. 43–54, 2002.